Evidence of growing bred vector associated with the tropical intraseasonal oscillation

Yoshimitsu Chikamoto,[1] Hitoshi Mukougawa,[1] Takuji Kubota,[2] Hitoshi Sato,[3] Akira Ito,[3] and Shuhei Maeda[3]

Received 12 October 2006; revised 10 January 2007; accepted 19 January 2007; published 20 February 2007.

[1] The stability property of the tropical intraseasonal oscillation (ISO) during 1 November 2003 to 31 January 2004 is examined using tropical bred vectors obtained from the operational numerical weather forecast system of the Japan Meteorological Agency. The tropical bred vectors are produced by a modified operational breeding cycle in which the perturbation is damped over the extratropics and rescaled by 3.3% of the climatological variance of the 200-hPa velocity potential in the tropics. At least two growing tropical bred vectors that have similar spatial structure to the observed dry Kelvin waves are obtained: dominant zonal wave number 1 components propagating eastward with phase speed of 30 m s^{-1}. The time-mean growth rate of the fastest growing tropical bred vector has a positive value of 0.1 day^{-1}. Although this growth rate is smaller than that of extratropical baroclinic instability, this result suggests that the tropical ISO is unstable to infinitesimal perturbations. **Citation:** Chikamoto, Y., H. Mukougawa, T. Kubota, H. Sato, A. Ito, and S. Maeda (2007), Evidence of growing bred vector associated with the tropical intraseasonal oscillation, *Geophys. Res. Lett.*, *34*, L04806, doi:10.1029/2006GL028450.

1. Introduction

[2] The tropical intraseasonal oscillation (ISO), known as the Madden-Julian Oscillation [e.g., *Madden and Julian*, 1994], is the most dominant component in the tropical intraseasonal variability in the troposphere. The tropical ISO is characterized by eastward propagating anomalous convective activity with a period of 30–60 days. The variation in convective activity associated with the tropical ISO accompanies the characteristic large-scale circulation anomaly, affecting the extratropical medium and extended range weather forecasts [*Waliser et al.*, 2003; *Jones et al.*, 2004]. However, the relationship between the predictability of the tropical ISO and tropical ISO activity is still controversial [*Boer*, 1995; *Jones et al.*, 2000; *Kubota et al.*, 2005]. Therefore, we have to use sophisticated method to evaluate the predictability of the tropical ISO.

[3] Ensemble prediction experiments provide one such useful technique to assess predictability of the tropical ISO [e.g., *Liess et al.*, 2005]. In the ensemble prediction experiments for the tropical ISO, we have to examine whether the specified initial perturbations are adequate for the tropical atmospheric motions. *Kubota et al.* [2005] indicated that initial perturbations produced by a Breeding of Growing Modes (BGM) method [*Toth and Kalnay*, 1993, 1997] in the operational ensemble prediction system of the Japan Meteorological Agency (JMA) are characterized by extratropical baroclinic unstable modes. In addition, kinetic energy of these initial perturbations in the tropical regions is too large for assessing the predictability of the tropical atmospheric circulation. This is because the norm of the initial perturbations in the operational BGM method of the JMA system is defined by the 500-hPa geopotential height variance. Thus, we modify the BGM method to create initial perturbations that are adequate to evaluate the predictability of the tropical ISO.

[4] In this paper, as a first step to evaluate the predictability of the tropical ISO, we will examine dynamical properties of initial perturbations obtained by a modified BGM method using the operational ensemble prediction system of the JMA. We modify several parts of the operational BGM method to create perturbations suitable for the tropical tropospheric circulation. As a result of this modification of the BGM method, growing perturbations associated with the tropical ISO are detected in the tropical regions, which suggests that the tropical ISO is linearly unstable to infinitesimal perturbations.

2. Modification of the BGM Method in JMA

[5] The operational JMA ensemble prediction system uses a global spectral model (JMA-GSM0305) with triangular 106 truncation (T106) and 40 vertical levels up to 0.4 hPa. A prognostic Arakawa-Schubert scheme [*Randall and Pan*, 1993] is implemented as the cumulus parameterization. In the numerical integration, the climatological daily mean sea surface temperature is prescribed and its anomalies are kept as constant values of the initial conditions. For further model details, the reader should consult *Japan Meteorological Agency* [2002].

[6] In the operational JMA ensemble weather prediction system, the initial perturbations are obtained by the BGM method as follows. At first, the model is integrated for 24 hours from the 6 perturbed and the unperturbed initial conditions. The differences between the unperturbed control and each of the perturbed 24 hour forecasts are orthonormalized by the Gram-Schmidt orthonormalization method using a specified norm of the perturbation. The norm is defined by using area-averaged root-mean square (RMS) variations of the 500-hPa geopotential height (Z_{500}) north of 20°S. The magnitude of the norm is set to be 14.5% of the

[1]Disaster Prevention Research Institute, Kyoto University, Kyoto, Japan.
[2]Department of Aerospace Engineering, Osaka Prefecture University, Osaka, Japan.
[3]Japan Meteorological Agency, Tokyo, Japan.

0094-8276/07/2006GL028450$05.00

climatological RMS Z_{500} variations. The orthonormalized perturbations are added to (or subtracted from) the analysis for the following day to create the next set of perturbations. The last step (the breeding cycle), i.e., the 24 hour forecast and the orthonormalization of the differences, is repeated to obtain initial perturbations for every day. The resulting set of orthonormal perturbations is mathematically related to the local Lyapunov vectors, and referred to as bred vectors. As *Toth and Kalnay* [1997] indicated, the spatial structure of the obtained leading bred vector is well characterized by baroclinic unstable modes since these modes have the largest growth rate in large-scale atmospheric motions. Thus, the operational breeding cycle of JMA is adequate to obtain growing errors in the extratropics associated with the baroclinic instability.

[7] In the tropical region, however, the amplitude of 200-hPa velocity potential (χ_{200}) of the bred vector of the JMA ensemble prediction system tends to be too large to assess the predictability of tropical atmospheric circulations [*Kubota et al.*, 2005]. Therefore, we have modified the operational breeding cycle of JMA to obtain suitable initial perturbations in the tropical region. First, the norm of the perturbation is defined by an area-averaged RMS χ_{200} variation in the tropical belt from 20°S to 20°N. Second, the magnitude of variables (X) associated with the initial perturbation of the breeding cycle is exponentially damped in the extratropics poleward of 20°S and 20°N as follows:

$$\begin{cases} X & \text{for } |\phi| \le 20^\circ \\ X \exp\{-(|\phi| - 20^\circ)^2/50\} & \text{for } |\phi| > 20^\circ \end{cases} \quad (1)$$

where ϕ is latitude. Since these tapered perturbations effectively reduce the vigorous baroclinic instability prevailing in the extratropics, we obtain perturbations related to the tropical atmospheric circulation. Third, each perturbation is normalized, i.e., rescaled every 24 hours but not orthogonalized, which is intended to check the existence of a growing unstable mode in the tropical regions. The magnitude of the norm is set to be 14.5%, 10%, 3.3%, 1%, 0.33%, and 0.1% of the climatological RMS χ_{200} variance. This is done in different breeding cycle runs in order to test the sensitivity of the bred vector with respect to the amplitude. We start the modified breeding cycles from 15 October 2003 for two random perturbations, and obtain two bred vectors for each magnitude of the norm. Although results only for the leading bred vector will be shown in the following section, the second bred vector has similar dynamical properties to the leading bred vector. The similarity between these two bred vectors also suggests the existence of an unstable mode. The analysis on the bred vectors was made during a period from 1 November 2003 to 31 January 2004 when active tropical ISO was observed.

3. Results

[8] First of all, we examined the dependence of dynamical properties of the bred vector on the magnitude of the norm, i.e., the rescaling factor. Figure 1 shows the relationship between the rescaling factor and the time-mean growth rate of the leading tropical bred vector $\mathbf{v}_1(t)$ for the period from 1 November 2003 to 31 January 2004. The leading bred vector $\mathbf{v}_1(t)$ is computed every 24 hours, i.e., $t = k\Delta t$ where k = 1, 2, 3,..., N and Δt = 1 day. For the analysis period, $k = 1 (k = N = 92)$ corresponds to 1 November 2003 (31 January 2004). The time-mean growth rate $\overline{\alpha}^{N\Delta t}$ during a period of $N\Delta t$ is defined by the following time average of a local in time growth rate α ($k\Delta t$) for 24 hours:

$$\overline{\alpha}^{N\Delta t} = \frac{1}{N}\sum_{k=1}^{N} \alpha(k\Delta t), \quad (2)$$

$$\alpha(k\Delta t) \equiv \frac{1}{\Delta t} \ln \frac{\| \mathbf{v}_1'((k+1)\Delta t) \|}{\| \mathbf{v}_1(k\Delta t) \|}. \quad (3)$$

Here, $\mathbf{v}_1(k\Delta t)$ is the normalized (rescaled) leading bred vector at $t = k\Delta t$, $\mathbf{v}_1'((k+1)\Delta t)$ the evolved bred vector at $t = (k+1)\Delta t$ from $t = k\Delta t$, and $\| \bullet \|$ the norm of a vector $\bullet$ defined by the χ_{200} RMS variance within the 20°S–20°N latitude belt. If we take the time-averaging period N in equation (2) to be infinite, and the time evolution of the perturbation is described by a set of linearized equations for the system, then $\overline{\alpha}^{N\Delta t}$ is independent of Δt and equal to the largest Lyapunov exponent. Bred vectors are equal to Lyapunov vectors in the limit of small amplitudes.

[9] The abscissa of Figure 1 denotes the magnitude of $\|\mathbf{v}_1(k\Delta t)\|$ for a range from 0.1% to 14.5% of the climatological RMS χ_{200} variance. Each error bar in Figure 1 indicates the standard deviation of $\overline{\alpha}^{N'\Delta t}$ for N' = 30 days, which is computed using all consecutive segments of 30 days from 1 November 2003 to 31 January 2004. When the rescaling factor is 3.3% of the climatological RMS χ_{200} variance, $\overline{\alpha}^{N\Delta t}$ of the leading bred vector has a positive value around 0.1 day^{-1}, corresponding to a doubling time of 7 days. This fact suggests the existence of a dynamically unstable mode associated with large-scale tropospheric motions although the growth rate of the tropical bred vector is considerably smaller than that of the extratropical bred vector. The growth rate of extratropical perturbations dominated by baroclinic unstable modes for 24 hours is 0.4 day^{-1} (cross mark in Figure 1). Increasing the rescaling factors to 10% and 14.5% decreases the growth rate of the leading bred vector slightly presumably due to the nonlinear effects, while the spatial structure of the bred vector is almost identical to that for the rescaling factor of 3.3% (not shown).

[10] On the other hand, when the rescaling factors are smaller than 1% of the climatological RMS χ_{200} variance, the growth rate increases enormously as the rescaling factor decreases. Previous studies pointed out that the fastest growing perturbations produced by the BGM method with considerably small rescaling factor are related to convective instability [*Toth and Kalnay*, 1997]. *Toth and Kalnay* [1997] showed that perturbations associated with the convective instability appear when the rescaling factor is set to be less than 1% of the climatological RMS variance of the 500-hPa stream function field. They also indicated that when the rescaling factor is reduced to less than 0.1% in the climatological RMS variance, the perturbation growth rate increases enormously. Therefore, it is plausible that the tropical bred vectors with the rescaling factors smaller than 1% are dominated by convective unstable modes. In fact, the tropical bred vectors less than 1% are dominated by an

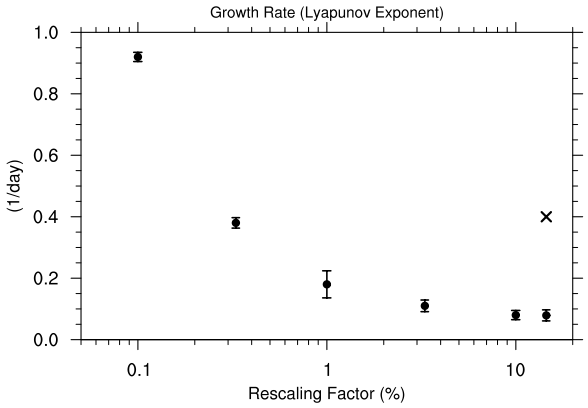

Figure 1. The time-mean growth rate of the leading tropical bred vector for a 92-day period with rescaling factors of 0.1%, 0.33%, 1%, 3.3%, 10%, and 14.5% of the climatological RMS variance of the 200-hPa velocity potential (see text). Solid circles (cross) indicate the time-mean growth rate of tropical (extratropical) bred vectors. Each error bar is estimated from the standard deviation of the time-mean growth rate for a 30-day period.

incoherent small-scale spatial structure, which is different from the situation for rescaling factors larger than 3.3% as we will see below. By choosing the appropriate variables, scaling amplitude, and scaling periods in the BGM method for the coupled general circulation model, *Yang et al.* [2006] also succeeded in isolating a slowly growing mode associated with the ENSO variability from baroclinic waves.

[11] Figure 2 shows snapshots of χ_{200} and χ_{850} (850-hPa velocity potential) associated with $\mathbf{v}_1(t)$ on 26 November 2003 obtained using rescaling factors of 3.3% and 0.33%. With the rescaling factor of 3.3%, a pattern of planetary-scale structure in the upper-level divergence and convergence appears over the tropical Atlantic and the central Pacific regions, associated with dominant zonal wave number 1 (WN1) components (Figure 2a). This upper-level perturbation pattern accompanies lower-level convergence and divergence over those regions (Figure 2b), exhibiting a vertical baroclinic structure. Similar planetary-scale structure is observed for the tropical bred vectors produced with rescaling factors of 10% and 14.5% (not shown). On the contrary, a rescaling factor of 0.33% destroys coherent structure with the prevailing WN1 component in the tropics (Figures 2c and 2d). Instead, a small-scale horizontal structure becomes dominant particularly over the central Pacific for $\mathbf{v}_1(t)$, which also suggests the predominance of the convective unstable mode for extremely small rescaling factors.

[12] Eastward phase propagation is another important feature of the leading tropical bred vector $\mathbf{v}_1(t)$. Figure 3 shows Hovmöller diagrams of χ_{200} averaged over the latitudinal band of 10°S–10°N for the observed field and for $\mathbf{v}_1(t)$ with the rescaling factors of 3.3% and 0.33%. The eastward propagation associated with the active phase of the observed tropical ISO becomes significant from December to early January (Figure 3a). In the following late January, the subsequent upper-level divergence and its eastward propagation associated with the tropical ISO are also observed over the Indian Ocean and the western Pacific. For the rescaling factor of 3.3%, eastward propagation with a phase speed of about 30 m s^{-1} (a period of about 15 days) dominated by WN1 components was frequently observed during this experimental period (Figure 3b). The eastward propagating bred vector slightly reduces its phase speed in December, but is still faster than the propagation of the tropical ISO. The eastward propagation of the bred vector begins over the Indian Ocean (30°E–90°E), and becomes prominent over the western Pacific (90°E–180°). In these regions, an eastward propagation of the tropical ISO is also most prominent [e.g., *Hsu and Lee* 2005]. In late January when the next active phase of the tropical ISO initiates over the Indian Ocean, the eastward propagation of the bred vector tends to be fast, and WN2 and WN3 components develop particularly over the Indian Ocean. For the rescaling factor of 0.33%, on the other hand, no significant eastward propagation is observed, while a standing oscilla-

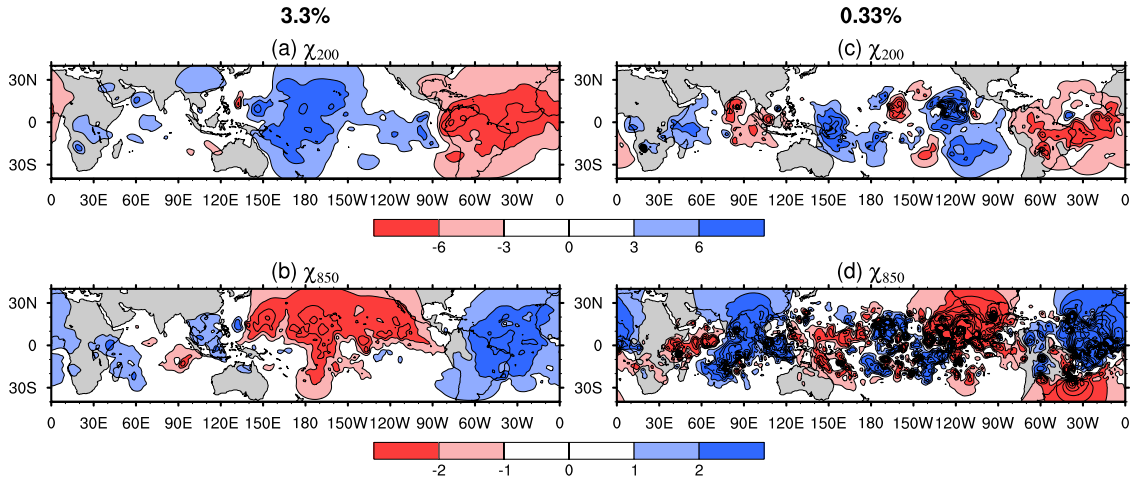

Figure 2. Snapshots of (a, b) 200-hPa and (c, d) 850-hPa velocity potential fields of tropical bred vectors on 26 November 2003. The left (right) plots show tropical bred vectors with rescaling factor of 3.3% (0.33%) of the climatological RMS variance of the 200-hPa velocity potential. Amplitudes of these bred vectors are normalized. Positive (negative) values indicate convergence (divergence). The contour intervals for the top (bottom) plots are 3×10^5 m^2 s^{-1} (1×10^5 m^2 s^{-1}).

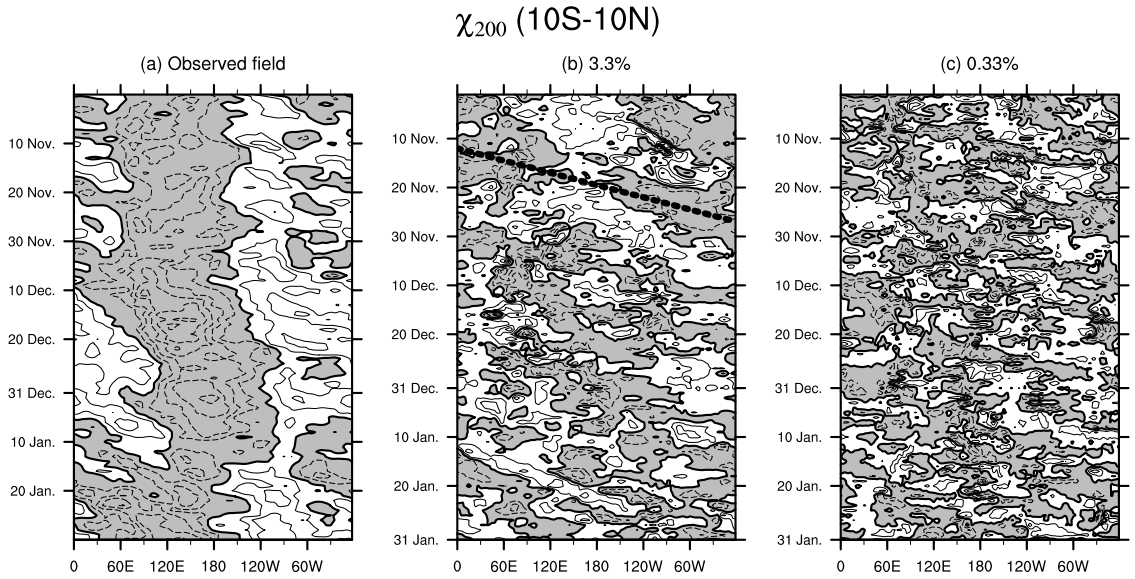

Figure 3. Hovmöller diagrams of 200-hPa velocity potential averaged over the 10°S–10°N region for (a) the observed field, (b) the bred vector for a rescaling factor of 3.3%, and (c) the bred vector for a rescaling factor of 0.33%. Amplitudes of these bred vectors are normalized. The contour interval at the left plot (center and right plots) is 5×10^6 m^2 s^{-1} (5×10^5 m^2 s^{-1}). Negative values (divergence) are shaded. Dotted line in Figure 3b indicates a phase line with speed of 30 m s^{-1}.

tion with small horizontal scale is dominant (Figure 3c). This fact also supports the predominance of the convective mode for the bred vector at 0.33% amplitude or smaller.

[13] To further examine the eastward propagation characteristics of $\mathbf{v}_1(t)$, we performed space-time spectral analysis [*Hayashi*, 1982] for the χ_{200} perturbation averaged over the latitudinal band of 10°S–10°N for the rescaling factors of 3.3% and 0.33% (Figure 4). For the rescaling factor of 3.3%, the eastward propagating WN1 component with a frequency of 0.04–0.08 cpd (a period of 12.5–25 days) has a spectral peak (Figure 4a). Another weak spectral peak is also seen in the frequency of eastward propagating WN2 components. A similar spectral peak is also obtained for $\mathbf{v}_1(t)$ with rescaling factors of 10% and 14.5% (not shown). For the rescaling factor of 0.33% (Figure 4b), however, the spectral peak is obscure and high-frequency modes with small zonal structure attain relatively large amplitude, which implies the dominance of the convective mode.

[14] By examining space-time spectral analysis for the zonal wind component at 200-hPa in the tropics associated with the leading bred vector for the rescaling factor of 3.3%, we also detect a broad spectral peak for the eastward propagating WN1 component with frequency of around 0.04 cpd. This spectral peak corresponds to the χ_{200} spectral peak although the horizontal pattern of the zonal wind component is not so organized as that of χ_{200}. For the meridional wind component, on the other hand, there is no apparent spectral peak. Thus, the leading bred vector has spatial structure similar to equatorial Kelvin waves as discussed later. Furthermore, the horizontal distribution of the precipitation associated with the leading bred vector is

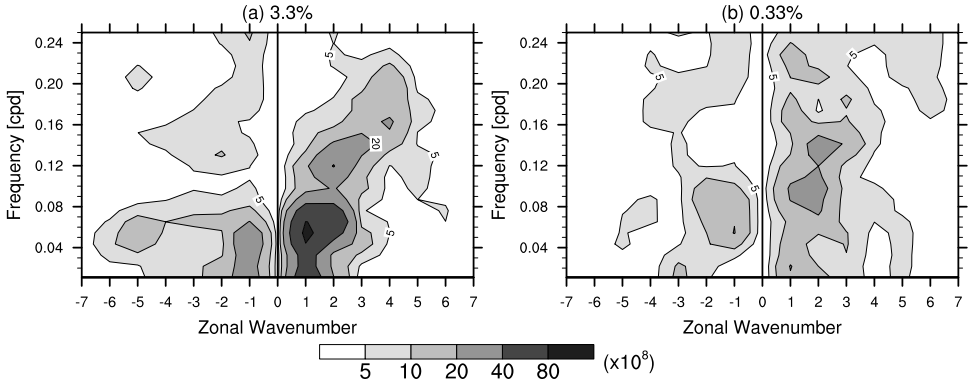

Figure 4. The space-time spectrum of the 200-hPa velocity potential of the tropical bred vector averaged over the 10°S–10°N region. The spectral power is smoothed with a 1-3-5-3-1 filter in frequency. The horizontal and vertical axes are zonal wave number and frequency (cycle per day), respectively. Positive (negative) zonal wave numbers indicate eastward (westward) propagation.

not related to the χ_{200} perturbation at all, suggesting that for the rescaling factor of 3.3% this mode is basically decoupled from the convection.

4. Discussion

[15] Our study based on the modified breeding cycle of the operational JMA ensemble prediction system reveals the existence of at least two growing tropical bred vectors with small but positive growth rates (0.1 day^{-1}) from 1 November 2003 to 31 January 2004. Since the tropical large-scale atmospheric circulation during this period is well characterized by dominant tropical ISO signals, the growing tropical bred vector could correspond to linearly unstable mode associated with the tropical ISO. Specifically, our results suggest that the tropical ISO is unstable to infinitesimal perturbations. Since the obtained doubling time of 7 days for the tropical bred vector is still short compared with the period of the tropical ISO, it could be possible to discuss the dependence of the growth rate on the phase of the tropical ISO.

[16] A critical caveat for the argument might be the reproducibility of the tropical ISO in the operational JMA weather forecast model. In fact, the forecast of the tropical circulation becomes unskillful beyond a lead time of 8 days for the JMA model [*Kubota et al.*, 2005]. However, the bred vectors obtained in our study are computed using the 1-day forecasts from the daily analysis with and without initial perturbations. Thus, our results would not suffer from the lack of forecast skill for the tropical ISO by the JMA prediction model with longer lead times.

[17] It is interesting to note that the obtained tropical bred vector tapered in the extratropics for the rescaling factors of 3.3%−14.5% has similar characteristics to the observed dry Kelvin waves in the tropics reported by previous studies [*Milliff and Madden*, 1996; *Bantzer and Wallace*, 1996]. The dry Kelvin wave is characterized by eastward propagating WN1 components with a phase speed of about 30 m s^{-1}, and has a vertical structure of the first baroclinic mode. *Milliff and Madden* [1996] proposed a conceptual model of the dry Kelvin waves as a far-field dispersion product of strong convection associated with the tropical ISO in the Indian Ocean and the western Pacific. This conceptual model would help us to understand the instability mechanism of the tropical ISO. Moreover, *Matthews et al.* [1999] indicated that the eastward propagating Kelvin waves over the equatorial Pacific are associated with enhanced convection over the Indian Ocean. Recently, *Hsu and Lee* [2005] suggested that the eastward propagation of the tropical ISO is caused by a combination of three equatorial Kelvin waves across the three ocean basins around the globe. Therefore, further analysis for the eastward propagating tropical bred vector is necessary to understand not only the instability mechanism but also the eastward propagating mechanism of the tropical ISO.

5. Conclusion

[18] Stability properties of the tropical ISO were examined by obtaining tropical bred vectors from the operational ensemble prediction system of the JMA from 1 November 2003 to 31 January 2004. The tropical bred vectors are derived from a modified breeding cycle in which the perturbations are damped over the extratropics beyond 20° and their norm is defined by the RMS variance of 200-hPa velocity potential (χ_{200}) in the tropics. When the prescribed magnitude of the norm is greater than 3.3% of the climatological RMS χ_{200} variance, at least two growing bred vectors with time-averaged growth rate of 0.1 day^{-1} are obtained. The growth rate of the tropical bred vectors is smaller than that of the baroclinic instability in the extratropics, but is clearly differentiated from the small-scale convective instability that dominates perturbation for extremely small magnitude of the norm. These tropical bred vectors are characterized by eastward propagating zonal wave number 1 components of the first baroclinic structure with a phase speed of about 30 m s^{-1}. Thus, our study suggests that the tropical ISO is unstable to infinitesimal perturbations.

[19] It is also interesting to note that those growing bred vectors have similar spatio-temporal characteristics with eastward propagating dry Kelvin waves detected by observational analysis [*Milliff and Madden*, 1996; *Bantzer and Wallace*, 1996]. This similarity might be a key to understand the instability mechanism associated with the tropical ISO. We are now conducting further analysis to reveal the instability mechanism of the tropical ISO and the dependence of the predictability of the tropical ISO on its phase and activity using the newly obtained bred vectors described in this study.

[20] **Acknowledgments.** We would like to thank M. Kyoda for the use of the BGM method in the JMA ensemble prediction system. The manuscript benefited from the constructive comments by E. Kalnay and an anonymous reviewer. This work was partly supported by KAGI21.

References

Bantzer, C. H., and J. M. Wallace (1996), Intraseasonal variability in tropical mean temperature and precipitation and their relation to the tropical 40–50 day oscillation, *J. Atmos. Sci.*, *53*, 3032–3045.

Boer, G. J. (1995), Analyzed and forecast large-scale tropical divergent flow, *Mon. Weather Rev.*, *123*, 3539–3553.

Hayashi, Y. (1982), Space-time spectral analysis and its applications to atmospheric waves, *J. Meteorol. Soc. Jpn.*, *60*, 156–171.

Hsu, H.-H., and M.-Y. Lee (2005), Topographic effects on the eastward propagation and initiation of the Madden-Julian Oscillation, *J. Clim.*, *18*, 795–809.

Japan Meteorological Agency (2002), Outline of the operational numerical weather prediction at the Japan Meteorological Agency (JMA), appendix to WMO numerical weather prediction report, p. 157, Tokyo.

Jones, C., D. E. Waliser, J. E. Schemm, and W. K. Lau (2000), Prediction skill of the Madden and Julian oscillation in dynamical extended range weather forecasts, *Clim. Dyn.*, *16*, 273–289.

Jones, C., D. E. Waliser, K. M. Lau, and W. Stern (2004), The Madden-Julian Oscillation and its impact on Northern Hemisphere weather predictability, *Mon. Weather Rev.*, *132*, 1462–1471.

Kubota, T., H. Mukougawa, and T. Iwashima (2005), Predictability of Madden and Julian oscillation in JMA one-month forecasts, *Ann. Disaster Prev. Res. Inst. Kyoto Univ., Ser. B*, *48*, 475–490.

Liess, S., D. E. Waliser, and S. D. Schubert (2005), Predictability studies of the intraseasonal oscillation with the ECHAM5 GCM, *J. Atmos. Sci.*, *62*, 3320–3336.

Madden, R. A., and P. R. Julian (1994), Observation of the 40–50 day tropical oscillation: A review, *Mon. Weather Rev.*, *122*, 814–837.

Matthews, A. J., J. M. Slingo, B. J. Hoskins, and P. M. Inness (1999), Fast and slow Kelvin waves in the Madden-Julian Oscillation of a GCM, *Q. J. R. Meteorol. Soc.*, *125*, 1473–1498.

Milliff, R. F., and R. A. Madden (1996), The existence and vertical structure of fast, eastward-moving disturbances in the equatorial troposphere, *J. Atmos. Sci.*, *53*, 586–597.

Randall, D. A., and D.-M. Pan (1993), Implementation of the Arakawa-Schubert cumulus parameterization with a prognostic closure, in *The Representation of Cumulus Convection in Numerical Models*, edited by K. A. Emanuel and D. J. Raymond, pp. 137–147, Am. Meteorol. Soc., Boston, Mass.

Toth, Z., and E. Kalnay (1993), Ensemble forecasting at NMC: The generation of perturbations, *Bull. Am. Meteorol. Soc.*, *74*, 2317–2330.

Toth, Z., and E. Kalnay (1997), Ensemble forecasting at NCEP and the breeding method, *Mon. Weather Rev.*, *125*, 3297–3319.

Waliser, D. E., K. M. Lau, W. Stern, and C. Jones (2003), Potential predictability of the Madden-Julian Oscillation, *Bull. Am. Meteorol. Soc.*, *84*, 33–50.

Yang, S.-C., M. Cai, E. Kalnay, M. Rienecker, G. Yuan, and Z. Toth (2006), ENSO bred vectors in coupled ocean-atmosphere general circulation models, *J. Clim.*, *19*, 1422–1436.

Y. Chikamoto and H. Mukougawa, Disaster Prevention Research Institute, Kyoto University, Gokasyo, Uji-shi, Kyoto 611-0011, Japan. (chika44@dpac.dpri.kyoto-u.ac.jp)

A. Ito, S. Maeda, and H. Sato, Japan Meteorological Agency, 1-3-4 Otemachi, Chiyoda-ku, Tokyo, 100-8122, Japan.

T. Kubota, 1-1 Gakuenmachi, Department of Aerospace Engineering, Osaka Prefecture University, Sakai, Osaka, 599-8531, Japan.